Basic Helix-Loop-Helix Transcription Factors Cooperate To Specify a Cortical Projection Neuron Identity[▽][†]

Pierre Mattar, Lisa Marie Langevin, Kathryn Markham, Natalia Klenin, Salma Shivji,
Dawn Zinyk, and Carol Schuurmans*

Institute of Maternal and Child Health, Hotchkiss Brain Institute, University of Calgary, Calgary, Alberta, Canada

Several transcription factors are essential determinants of a cortical projection neuron identity, but their mode of action (instructive versus permissive) and downstream genetic cascades remain poorly defined. Here, we demonstrate that the proneural basic helix-loop-helix (bHLH) gene *Ngn2* instructs a partial cortical identity when misexpressed in ventral telencephalic progenitors, inducing ectopic marker expression in a defined temporal sequence, including early (24 h; *Nscl2*), intermediate (48 h; *BhlhB5*), and late (72 h; *NeuroD*, *NeuroD2*, *Math2*, and *Tbr1*) target genes. Strikingly, cortical gene expression was much more rapidly induced by *Ngn2* in the dorsal telencephalon (within 12 to 24 h). We identify the bHLH gene *Math3* as a dorsally restricted *Ngn2* transcriptional target and cofactor, which synergizes with *Ngn2* to accelerate target gene transcription in the cortex. Using a novel in vivo luciferase assay, we show that *Ngn2* generates only ~60% of the transcriptional drive in ventral versus dorsal telencephalic domains, an activity that is augmented by *Math3*, providing a mechanistic basis for regional differences in *Ngn2* function. Cortical bHLH genes thus cooperate to control transcriptional strength, thereby temporally coordinating downstream gene expression.

Advanced cognitive functioning is controlled by the cerebral cortex, which includes the six-layered neocortex, a brain region mainly comprised of excitatory, glutamatergic projection neurons and a smaller number of inhibitory, GABAergic (where GABA is γ-aminobutyric acid) interneurons. While all cortical projection neurons share a pyramidal morphology, dorsal telencephalic origin, and glutamatergic neurotransmitter phenotype, they also display laminar and region-specific differences in morphology, projection pattern, and gene expression (47, 57). The homeodomain transcription factors *Lhx2*, *Pax6*, and *Emx2* are considered cortical selector genes as they are each required for cortical development (48, 49). Strikingly, in *Pax6*; *Emx2* double mutants, the neocortex is converted to basal ganglia, a ventral telencephalic territory (49). A similar conversion of dorsal (cortical) to ventral regional identity also occurs in mice carrying mutations in β-*catenin* and *Gli3*, downstream transcriptional effectors in the Wnt and Shh signaling pathways, respectively (6, 72, 73). Moreover, ventral, GABAergic rather than dorsal, glutamatergic neurons differentiate in *Ngn2* mutant cortices, a proneural gene encoding a basic-helix-loop-helix (bHLH) transcription factor (19, 62). Taken together, these studies demonstrate that the decision to differentiate into a glutamatergic versus GABAergic neuronal phenotype is a binary fate choice in the telencephalon, a phenomenon that is also observed in the thalamus, midbrain, and spinal cord (16, 50, 56, 62).

Gain-of-function studies can determine if genes act permissively or instructively to specify neuronal phenotypes. In the telencephalon, misexpression of *Wnt* pathway effectors has dorsalizing effects both in vitro and in vivo (6, 24, 42, 76). In addition, *Emx1* and *Emx2* are sufficient to convert medial telencephalic territories destined to form choroid plexus into cortex (75). Unexpectedly, overexpression of *Pax6* inhibits rather than promotes neuronal differentiation, and while *Pax6* can upregulate some cortex-specific genes when overexpressed in the cortex, it remains to be determined if it plays an instructive role in specifying cortical neuronal identities when misexpressed in ectopic sites (4, 10, 29). Likewise, it remains to be determined if *Wnt* pathway effectors and *Emx* genes only initiate the transcription of cortical progenitor genes or also induce markers of a mature projection neuron identity.

The proneural functions of the *Ngn* genes have been examined in various vertebrate species, revealing a role for these transcription factors in the induction of generic neuronal differentiation (14, 32, 33, 53, 55, 60). Specifically, the *Ngn* genes are thought to promote differentiation by inducing the expression of cascades of effector bHLH genes (66). Indeed, in the neocortex, as neuronal precursors differentiate, they initiate the expression of a number of such bHLH genes, including *Ngn1/Ngn2*, *Math2*, *Math3*, *NeuroD*, *NeuroD2*, *Nscl1*, *Nscl2*, and *Bhlhb5*. While mutations in most of these bHLH genes have been reported (with the exception of *Bhlhb5*), defects in the specification of cortical neurons have been shown only in *Ngn1/Ngn2* mutants (19, 62). The lack of similar defects in other bHLH mutants may reflect either a later role for some of these factors or redundant functions between bHLH genes that share expression domains, as demonstrated in other systems (35, 74). Indeed, *NeuroD2* is required postnatally for the survival of cortical neurons, while *NeuroD2* and *Math2* cooperate to regulate differentiation and survival of hippocampal granule neurons (34, 40, 51, 64, 65, 74).

In addition to specifying generic neuronal differentiation, the proneural genes have been implicated in the specification

of neuronal subtype identities (63). However, while the *Ngn* genes act permissively to specify identities in some neural lineages, there are also examples whereby the *Ngn* genes are instructive for neuronal fate (31, 41, 53, 54, 60). To determine how *Ngn2* specifies a glutamatergic projection neuron fate in the cortex, we misexpressed *Ngn2* in the dorsal and ventral telencephalon via in utero electroporation (36, 59). Here, we show that *Ngn2* is sufficient to induce a cascade of cortical gene expression in a temporally defined order in the ventral telencephalon, demonstrating that *Ngn2* is partially instructive for a projection neuron identity. Furthermore, we implicate *Math3* as a key cofactor in the *Ngn2*-regulated cortical differentiation cascade, demonstrating that *Ngn2* and *Math3* cooperate to temporally coordinate the onset of cortical gene transcription.

MATERIALS AND METHODS

Animals. Embryos were staged using the morning of the vaginal plug as embryonic day 0.5 (E0.5). CD1 mice (Charles River) were used for in utero electroporation experiments. *Ngn2* mutant lines in which a *GFP* cassette was knocked into the *Ngn2* locus were maintained as heterozygotes on a CD1 background, and genotyping was performed as described previously (12).

In utero electroporation. Previously described *Ngn2NRAQ* (38), *NeuroD* (37), and *Math3* (70) cDNAs were subcloned into the pCIG2 expression vector (26) using standard procedures. *Ngn2* cDNA was subcloned into pCIG2 by PCR amplification from an E13.5 murine cDNA library using the primers Ngn2F (GTGTGTGAATTCGTAGGATGTTCGTCAA) and Ngn2R (GTGTGTGAA TTCCTCTAGATACAGTCC). Electroporations were performed at E12.5 as described previously (12, 36, 59) using column-purified endotoxin-free DNA (Qiagen) and platinum tweezer-style electrodes (5 mm; Protech) to apply seven 30-mS pulses at 50 V.

RNA in situ hybridization. Electroporated brains were fixed overnight in 4% paraformaldehyde, dissolved in diethylpyrocarbonate-treated phosphate-buffered saline (PBS), serially cryosectioned at 10 μm, and collected on Superfrost Plus (Fisher) slides. Slides were processed for RNA in situ hybridization as described previously (2, 12). Probes were used for the following genes (gene aliases are given in parentheses): *EGFP* (Cairine Logan, University of Calgary), *Ngn2* (*Neucog2/Math4a*) (22), *Mash1* (*ascl1*) (23), *Math2* (*NeuroD6/Nex*) (7), *Math3* (*NeuroD4/ath3/NeuroM*) (70), *NeuroD* (*NeuroD1*) (37), *Nscl1* (*Nhlh1/Hen1/Tal2*) (8), *Nscl2* (*Nhlh2/Hen2*) (C. Glenn Begley, Amgen Inc.), *Bhlhb5* (*Beta3*) (77), *Id2* (*Idb2*) (25), *Tbr1* (27), *VGlut2* (*Slc17a6*) (20), *GAD1* (*GAD67*) (9), *Mef2c* (43), *Pax6* (68), *FezL* (*FezF2/Zfp312*) (28), *Robo1* (*Dutt1*) (3), and *RORβ* (*RZRβ/Nr1f2*) (61). A *NeuroD2* (*Ndrf*) probe was generated from an IMAGE Consortium (Lawrence Livermore National Laboratory) cDNA clone from Open Biosystems (Hunstville, AL) (IMAGE clone 6817440; GenBank accession no. BC058965).

Immunostaining and imaging. Slides were processed for immunostaining as described previously (2, 12). Primary antibodies included mouse anti-NeuN (1/500; Chemicon, Temecula, CA), mouse anti-β-III-tubulin (1/500; Swant, Bellinzona, Switzerland), rabbit anti-green fluorescent protein (anti-GFP; 1/500; Chemicon), rabbit anti-ER81 (1/500; Tom Jessell and Susan Morton [5]), goat anti-NeuroD (1:100; Santa Cruz Biotechnology, Santa Cruz, CA), mouse anti-Ngn2 (1/4; David Anderson [41]), rabbit anti-Tbr1 (1:3,000; Chemicon), goat anti-Bhlhb5 (1:1,000; Santa Cruz), and rabbit anti-Otx1 (1/500; Flora Vaccarino [39]). Secondary antibodies were conjugated to Cy3, aminomethylcoumarin acetate (Jackson Immunoresearch, West Grove, PA) or Alexa488 (Molecular Probes) and diluted 1/500. Some sections were stained for 5 min with 4′,6-diamidino-2-phenylindole (DAPI; 1/10,000 dilution in 1× PBS; Santa Cruz), washed an additional three times with PBS, and mounted with AquaPolymount (Polysciences, Inc., Warrington PA). Bright-field and fluorescence microscopy was performed as described previously (12). The numbers of informative brains examined are shown in the figures (see Fig. 4 to 6, lower-right corners of panels; see also Fig. S5 in the supplemental material). Double in situ hybridization was performed as described previously (67). For cell counts of immunostained sections, the number of GFP-positive cells that coexpressed the marker of interest were enumerated from two to three sections from at least three independently transfected brains. For ventral transfections, the minimum number of GFP-positive cells counted per experimental group was 1,257 (range, 1,257 to 1,808), while in dorsal transfections the total number of cells counted was 1,767.

Luciferase assays. P19 cells (American Type Culture Collection) were transfected with a combination of the B1-1000 *NeuroD* luciferase plasmid (30) and the pβ-*actin-lacZ* plasmid at 0.5 μg/μl and 0.1 μg/μl, respectively, for P19 cell transfections and at an equivalent ratio of 1 μg/μl each for in vivo electroporations of the telencephalon. P19 cells were cultured in alpha minimal essential medium supplemented with L-glutamine and ribonucleosides (Invitrogen, Burlington, Ontario, Canada), to which sodium bicarbonate, penicillin/streptomycin, and 10% fetal bovine serum (Invitrogen) were added. For luciferase experiments, P19 cells were seeded into six-well plates at 100,000 cells per well and transfected with Lipofectamine Plus (Invitrogen) according to the manufacturer's instructions. Luciferase assays were performed using Reporter Lysis Buffer and Luciferase Assay System (Promega, Madison WI) according to the manufacturer's protocol. For electroporated tissue, samples were placed in a microcentrifuge tube with 100 μl of Reporter Lysis Buffer and triturated with a 200-μl pipette tip before being subjected to freeze-thaw cycles. To detect β-galactosidase enzyme activity, fixed volumes (10 or 50 μl) of lysate were suspended in 500 μl of 5-bromo-4-chloro-3-indolyl-β′-D-galactopyranoside buffer (PBS, pH 7.0, with 2 mM MgCl$_2$ and 50 mM β-mercaptoethanol), to which 400 μg (in 100 μl of double-distilled H$_2$O) of o-nitrophenyl-β-D-galactopyranoside (Rockland, Gilbertsville, PA) was added. Samples were incubated for 1 to 16 h, and absorbance at 420 nm was analyzed in a Beckman DU 640 spectrophotometer. Data were normalized by dividing raw light units by the corresponding A_{420} values. To make specific comparisons between two sample sets in our in vivo luciferase studies, statistical analyses were performed using a Wilcoxon *t* test (Wilcoxon signed rank test). For luciferase assays in P19 cells, multiple comparisons were performed by applying a one-way analysis of variance and Tukey's multiple comparison test. Both tests were applied using Graphpad Prizm software (San Diego, CA).

GST pull-down assays. To generate pGex2T-*Ngn2*, the *Ngn2* open reading frame was excised from pCIG2-*Ngn2* using EcoR1 and ligated into the EcoR1 site of pGex2T (Pharmacia). To subclone *Math3* into EcoRI-linearized pBluescript II KS (Stratagene), the open reading frame was amplified by PCR from pCIG2-*Math3* using the primers Math3S (GAGAGAATTCGATGGCAAAAATGTATATG) and Math3AS (GAGAGAATTCCTAATCAGAGAAGATCGTATTG), cut with EcoR1, and ligated with standard conditions. ^{35}S-labeled Math3 and E47 proteins were generated using Express Protein Labeling Mix (Perkin Elmer) and a TNT Coupled Reticulocyte Lysate System (Promega) using the pBluescript-*Math3* and pcDNA3-*E47* plasmids as templates. Glutathione *S*-transferase (GST) pull-down assays were performed as described previously (22). Densitometry was performed on scanned images using Adobe Photoshop software.

RESULTS

Identification of candidate *Ngn2* target genes in the cortex. In *Drosophila*, proneural genes activate transcriptional cascades composed of bHLH and non-bHLH transcription factors (11), as do bHLH determination genes in vertebrate skeletal muscle (52). To characterize the cortical transcriptional cascade(s) executed downstream of *Ngn2*, we selected a panel of potential target genes using restricted or enriched expression in the dorsal telencephalon and deregulated expression in *Ngn2* mutant cortices as criteria (19, 44, 62). At E13.5, *Ngn2* was expressed in the ventricular zone (VZ) of the dorsal and not ventral telencephalon (Fig. 1A) (19, 21, 22, 26). Of the other cortical bHLH genes, *Math3* expression was also confined to the VZ (Fig. 1B), while *NeuroD* was expressed in the subventricular zone (SVZ), a secondary population of cortical progenitors and newborn neurons (Fig. 1C). *Nscl1* was weakly expressed in the medial-most preplate, a layer containing the first postmitotic neurons in the cortex (Fig. 1D), while the related gene *Nscl2* was more robustly expressed throughout the preplate as well as at lower levels in the SVZ (Fig. 1E). *BhlhB5*, *NeuroD2*, and *Math2* were primarily expressed in the developing cortical plate, which is populated by later-born neurons (Fig. 1F to H). Of the non-bHLH genes, *VGlut2*, a glutamatergic marker, was expressed in the E13.5 SVZ and preplate (Fig. 1I), as was the T-box gene *Tbr1*, which was also expressed in the cortical plate (Fig. 1J). The zinc finger gene
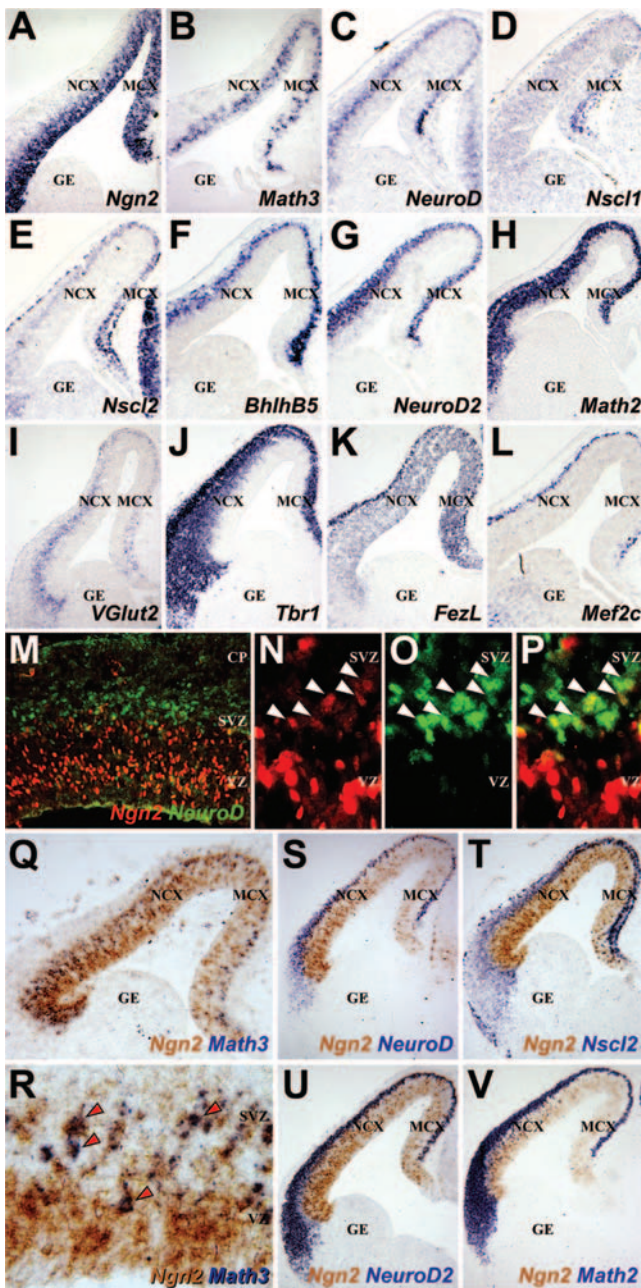
FIG. 1. Expression profiles of putative *Ngn2* target genes in the telencephalon. (A to L) RNA in situ hybridization of frontal sections of E13.5 brains with probes for *Ngn2*, *Math3*, *NeuroD*, *Nscl1*, *Nscl2*, *BhlhB5*, *NeuroD2*, *Math2*, *VGlut2*, *Tbr1*, *FezL*, and *Mef2c* (as labeled on panels). (M to P) Double immunolabeling of E13.5 cortex with anti-Ngn2 (red) and anti-NeuroD (green). Arrowheads mark double-positive cells at the VZ/SVZ border. (Q to V) Double in situ hybridization of frontal sections through the E12.5 telencephalon with probes for *Ngn2* (brown) in combination with probes for (all in purple; identified on panels) *Math3* (arrowheads mark double-positive cells, *NeuroD*, *Nscl2*, *NeuroD2*, or *Math2*. NCX, neocortex; MCX, medial cortex; CP, cortical plate.

FezL was expressed in the VZ and preplate (Fig. 1K) and was selected as a putative *Ngn2* target gene as it is required to specify subplate and layer V neurons (15, 28, 46), as is *Ngn2* (62). Finally, *Mef2c* (Fig. 1L) was analyzed as a nonregional-

ized, *Ngn2*-regulated, cortical gene (44), expressed dorsally in the preplate and cortical plate and ventrally in the ganglionic eminences (GE). With the exception of *FezL*, all of these genes have been previously reported to exhibit reduced expression in dorsomedial domains of *Ngn2* mutant cortices, results that we have reproduced in E13.5 *Ngn2* mutants for the purposes of clarity (see Fig. S1 in the supplemental material) (19, 44, 62). Importantly, *Math3* expression was completely lost in E13.5 *Ngn2* mutant cortices, at least at the level of detection afforded by RNA in situ hybridization (see Fig. S1B and B′ in the supplemental material), while other bHLH genes were less severely affected, due in part to the retained expression of *Ngn1* (data not shown), a related gene that was previously reported to have overlapping functions with *Ngn2* (19).

Math3 and *NeuroD* are direct transcriptional targets of *Ngn* genes in *Xenopus* (71). We reasoned that if *Math3* and/or *NeuroD* were direct *Ngn2* targets in the cortex, double-positive cells should be evident. While the vast majority of E13.5 cortical cells expressed only Ngn2 or NeuroD protein, a layer of double-positive cells one to two cells thick was observed at the VZ/SVZ interface (Fig. 1M to P). Similarly, using two-color RNA in situ hybridization, *Ngn2* and *NeuroD* transcripts colocalized at the E13.5 VZ/SVZ border but were exclusive elsewhere in the cortex (Fig. 1S). In striking contrast, most *Math3*-positive cells positioned in the upper VZ coexpressed *Ngn2* (Fig. 1Q and R). Finally, while the dorsoventral expression limits of the remaining bHLH genes registered precisely with those of *Ngn2* (Fig. 1Q to V), *Ngn2* displayed limited coexpression with *Nscl2*, *NeuroD2*, and *Math2*, with double-positive cells concentrated at the VZ/SVZ interface (Fig. 1T to V), while *Ngn2* and *BhlhB5* were not detectably coexpressed (data not shown). *Math3*, *NeuroD*, *Nscl2*, *NeuroD2*, and/or *Math2* could thus be direct transcriptional targets of *Ngn2*, albeit (with the exception of *Math3*) in a limited number of cells.

Ngn2 induces expression of a subset of dorsal regional markers in the ventral telencephalon. To understand how *Ngn2* executes its neuronal specification functions in the cortex, we used a gain-of-function approach. *Ngn2* was misexpressed in E12.5 telencephalic progenitors via in utero electroporation (36, 59) using a bicistronic expression vector for *Ngn2* and an internal ribosome entry site 2-enhanced GFP (EGFP) cassette (pCIG2 [26]). At E12.5, the telencephalon, which is a bilateral structure located in the rostral-most region of the embryonic neural tube (Fig. 2A, blue structures), has a large fluid-filled ventricle where DNA constructs were introduced with micropipettes. To target the uptake of DNA expression constructs into the dorsolateral telencephalon, electrodes were placed parallel to the E12.5 head in utero (Fig. 2A and B) (36, 59). With this approach, dorsal telencephalic progenitors, which line the ventricular surface, were preferentially targeted, while only a small number of ventral progenitors in the lateral GE were transfected (Fig. 2C, C′, D, and D′). To increase the number of ventral progenitors targeted, the cathode was rotated ~30° rostrally (Fig. 2E and F), resulting in reliable transfection of the E12.5 lateral GE and to a lesser extent the medial GE (83.2% electroporations with ventral cells targeted; n = 94/113) (Fig. 1G and G′). In sections taken through the telencephalon 24 h postelectroporation, typically, a continuum of dorsolateral (cortical) and ventral progenitors was electroporated (71.7% electroporations; n = 81/113) (Fig.

FIG. 2. *Ngn2* instructs a partial cortical, neuronal identity in the ventral telencephalon. (A and B) Schema of electroporation strategy to target dorsolateral cortex. (C and D) Example of E12.5 brain electroporated with pCIG2 at E12.5 and harvested 24 h later, showing whole-mount and opened views of dissected brain in bright-field (C and D) and fluorescence (C′ and D′) images, respectively. A small number of transfected GE cells are shown in the inset in panel D′. (E and F) Schema of electroporation strategy to target ventral telencephalon. (G and G′). Bright-field (G) and fluorescence (G′) images of dissected and opened brain electroporated at E12.5 and harvested 24 h later. (H) *EGFP* expression in electroporated E12.5 brain harvested after 24 h. Schematic in upper right corner shows a frontal section through the entire telencephalon, with the boxed area highlighting the location of the field in which *EGFP* expression is highlighted. (I to W) E12.5 brain electroporated with pCIG2-*Ngn2* and harvested at E16.5. Ventral views of bright-field (I) and fluorescence (J and J′) images. Panel J′ is a higher magnification image of boxed area in panel J. Dashed lines indicate the approximate locations of the sections depicted in (K to Y). (K to W) Frontal sections through electroporated ventral telencephalon imaged for EGFP epifluorescence (green) and BhlhB5 (red; K to M), NeuroD (red; N to P), Tbr1 (red; Q to W), and Ngn2 (blue; V and W) immunostaining. Double-positive cells are marked by arrowheads (L, M, and O to R). An untransfected, contralateral hemisphere immunostained with Tbr1 (S) is also shown. (X and Y) Frontal section through an electroporated E12.5 ventral telencephalon transfected with an empty pCIG2 vector and imaged for EGFP epifluorescence (green; Y) and Tbr1 (red; X and Y) expression at E16.5. Mes, mesencephalon; Di, diencephalon; Tel, telencephalon; LGE, lateral ganglionic eminence; MGE, medial ganglionic eminence; CGE, caudal ganglionic eminence; NCX, neocortex; LCX, lateral cortex; TH, thalamus; OB, olfactory bulb; LCS, lateral cortical stream.
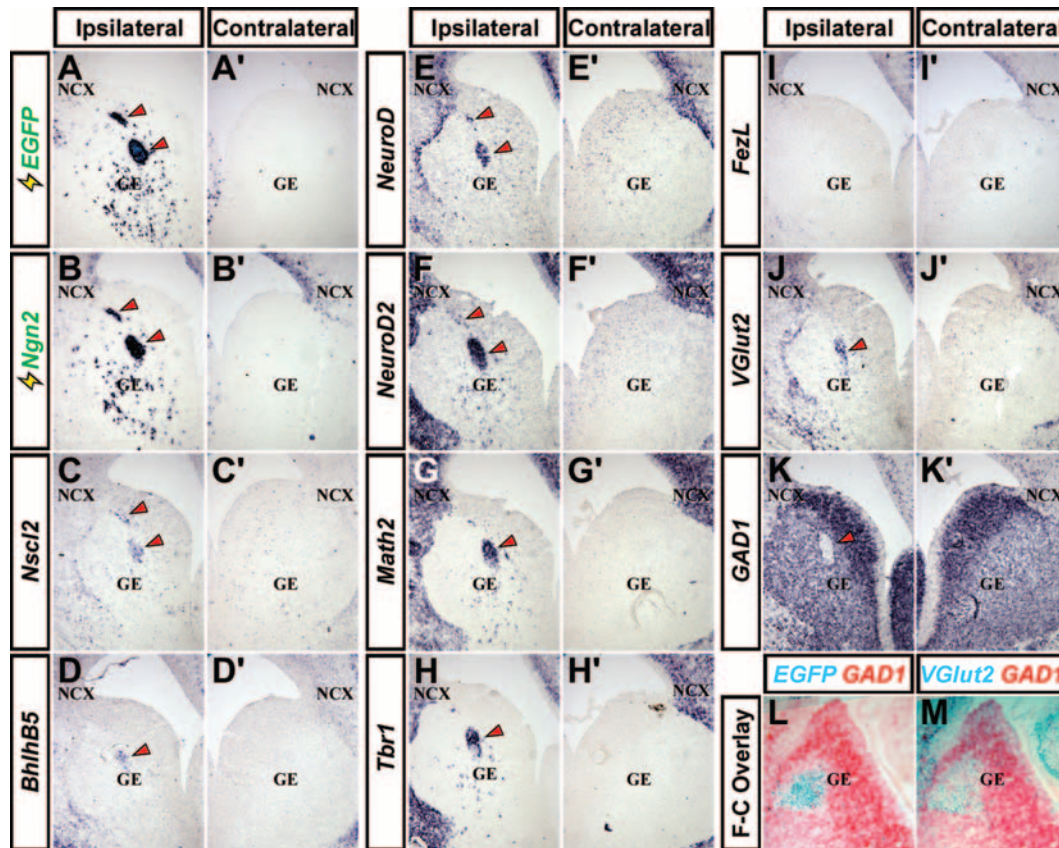
FIG. 3. Identification of *Ngn2* target genes in the ventral telencephalon. Frontal sections of E16.5 brain that was electroporated at E12.5 with pCIG2-*Ngn2*. Localizations are shown of transcripts for the *EGFP*, *Ngn2*, *Nscl2*, *BhlhB5*, *NeuroD*, *NeuroD2*, *Math2*, *Tbr1*, *FezL*, *VGlut2*, and *GAD1* genes (identified along left sides of panels). The contralateral hemisphere was not transfected (A′ to K′). (L and M) False-color overlay between adjacent sections hybridized with probes for *GAD1* (red) and EGFP (cyan; L) or *VGlut2* (cyan; M). Arrowheads mark ectopic gene expression (A to H, J, and K). NCX, neocortex.

2H), while only 16.8% (19/113) and 11.5% (13/113) of the electroporations, respectively, exclusively targeted dorsal or ventral cells.

To determine if *Ngn2* could induce ectopic cortical gene expression ventrally, embryos electroporated at E12.5 were harvested after 96 h, and successful transfection of the ventral telencephalon was identified by EGFP epifluorescence (Fig. 2I, J, and J′). In sections, EGFP-positive cells were scattered throughout the GE (Fig. 2K, M, N, and P), although in well-transfected brains, EGFP-positive cells instead aggregated together to form distinct heterotopia (Fig. 2Q to W and 3). Strikingly, a subset of EGFP-positive cells in the GE ectopically expressed the cortical-specific markers BhlhB5 (Fig. 2K to M), NeuroD (Fig. 2N to P) and Tbr1 (Fig. 2Q, R, T, and W). Tbr1 (Fig. 2S) and other cortical markers (data not shown) were not expressed in the nontransfected, contralateral GE. Ngn2 protein was also detected in EGFP-positive cells (Fig. 2V and W), while ectopic *Ngn2* transcripts were detectable up to 288 h posttransfection (longest time point analyzed) (see Fig. S2 in the supplemental material), indicating that *Ngn2* expression was maintained. *Ngn2* is thus sufficient to cell-autonomously instruct some aspects of cortical identity in the ventral telencephalon.

To determine if *Ngn2* was sufficient to initiate the expression of all or only a subset of cortical genes, we expanded the number of markers analyzed by using RNA in situ hybridization. Riboprobes for *EGFP* (Fig. 3A) and *Ngn2* (Fig. 3B) identified patches of *Ngn2*-transfected cells in the GE 96-h postelectroporation of the E12.5 telencephalon. In adjacent sections, genes ectopically induced by *Ngn2* in the GE included *Nscl2*, *BhlhB5*, *NeuroD*, *NeuroD2*, *Math2*, and *Tbr1* (Fig. 3C to H). In contrast, the dorsally restricted genes *Math3* (data not shown) and *FezL* (Fig. 3I) and the nonregionalized gene *Mef2c* (data not shown) were not induced by *Ngn2* in the GE (see Table S1 in the supplemental material). Verifying the specificity of gene induction by *Ngn2*, cells in the nontransfected, contralateral GE never expressed cortical genes (Fig. 3C′ to H′). Moreover, GE transfected with pCIG2, expressing EGFP alone (*n* = 15) (Fig. 2X and Y; see also Fig. S3 in the supplemental material) or *Ngn2* with a mutated, nonfunctional DNA-binding domain (*Ngn2NRAQ*; *n* = 2) (see Fig. S4 in the supplemental material) failed to induce ectopic cortical markers. Thus, although *Ngn2* can elicit some biological effects through DNA-binding-independent mechanisms (69), DNA binding is required to instruct a cortical identity.

***Ngn2* is instructive for neurotransmitter but not laminar identity.** We next questioned if *Ngn2* was sufficient to specify neurotransmitter and layer-specific phenotypes, which are per-

turbed in *Ngn* mutant cortices (19, 62). In brains electroporated at E12.5 and harvested 96 h later, *Ngn2*-expressing GE cells ectopically expressed *VGlut2* (Fig. 3J), which was not expressed in the nontransfected, contralateral GE (Fig. 3J′) or in control (empty vector or *Ngn2NRAQ*) electroporated GE cells (see Fig. S3 and S4 in the supplemental material). Concomitantly, *GAD1* expression was lost in *Ngn2*-transfected patches (Fig. 3K). Accordingly, the superimposition of adjacent sections showed that GE cells expressing *EGFP* (Fig. 3L), and hence *Ngn2* (not shown) and *VGlut2* (Fig. 3M), did not express *GAD1* (Fig. 3L). These data support the notion that glutamatergic traits are acquired at the expense of GABAergic phenotypes.

Ngn2 is required to specify the identities of early-born, deep-layer neurons (62). To test if *Ngn2* was sufficient to specify a deep-layer V/VI identity, we electroporated the dorsal telencephalon with *Ngn2* or control (*EGFP*) constructs at E14.5, when neurons in upper layers II to IV are born (36). Three days postelectroporation, *Ngn2*-transfected cells, including neurons that had reached the cortical plate, did not ectopically express Otx1 or ER81, layer V/VI and V markers, respectively (see Fig. S2 in the supplemental material). Similarly, at postnatal day 7, when cortical migration is complete, neurons derived from both *Ngn2*- and control-transfected E14.5 progenitors predominantly localized to layer IV and expressed appropriate layer markers (*ROR*β, *Bhlhb5*, and low *Tbr1*), while deep-layer markers (*FezL*, *Robo1*, and *ER81*) were not ectopically expressed (see Fig. S2 in the supplemental material). Finally, in ventral GE electroporations, deep-layer markers, including *Robo1*, *ER81*, and *Otx1*, were not induced by *Ngn2* (data not shown). *Ngn2* is thus sufficient to specify aspects of a dorsal regional and glutamatergic neurotransmitter identity but cannot impart neocortical layer properties.

Ordering the *Ngn2*-dependent genetic cascade. To examine the order of gene induction downstream of *Ngn2*, the stage of electroporation was kept constant (E12.5) while the time of analysis (6, 9, 12, 24, 48, and 72 h postelectroporation) was varied (see Table S1 and Fig. S5 in the supplemental material for a summary). Between 6 to 12 h posttransfection, no cortical genes were ectopically expressed in *Ngn2*-electroporated GE cells at levels detectable by RNA in situ hybridization. However, by 24 h, ectopic *Nscl2* transcripts were detected in the GE (*n* = 6/8 embryos) (Fig. 4C and E). *Nscl2* expression was maintained in *Ngn2*-transfected cells in the GE at 48 h postelectroporation in 4/4 embryos (Fig. 4C′), at which time, transcripts for *BhlhB5* were also apparent (3/5 embryos) (see Fig. S5C′ in the supplemental material). By 72 h, in addition to *Nscl2* (5/5 embryos) and *Bhlhb5* (4/4), ectopic expression of *NeuroD2* (3/3), *Math2* (2/2), *NeuroD* (4/4), *Tbr1* (3/3), and *VGlut2* (2/2) was readily apparent in all *Ngn2*-electroporated GE (Fig. 4A″ to D″; see also Fig. S5C″ to G″ in the supplemental material). Notably, all of the cortical genes analyzed were not expressed in the nontransfected contralateral GE or in control transfections, indicating that ectopic gene expression is a consequence of *Ngn2* misexpression (Fig. 4A‴ to D‴; see Fig. S3, S4, and S5C‴ to G‴ in the supplemental material). *Ngn2* thus induces cortical gene expression in a temporally defined manner in the GE (Fig. 4E).

***Ngn2* rapidly induces cortical gene expression in the neocortex.** We next tested if *Ngn2* could induce premature expression of cortical genes when misexpressed in the E12.5 dorsal telencephalon. At 12 h postelectroporation, *Ngn2*-misexpressing cells in the cortical VZ prematurely expressed *Nscl2* (3/8 brains) and *NeuroD* (6/8), while transcripts for genes induced later in the GE, such as *BhlhB5* (1/6) and *Tbr1* (1/6), were induced less frequently (data not shown; see Table S1 in the supplemental material). At 24 h postelectroporation, in strongly transfected cortices, *Ngn2* frequently induced the formation of columnar structures in the cortical VZ that were comprised of ectopic neurons positive for NeuN (columns formed in 5/10 brains; 5/5 columns were NeuN positive) (Fig. 5A and B), Tbr1 (Fig. 5C and D), and Tuj1 (data not shown). In *Ngn2*-induced cortical columns, the precocious expression of *Math3* (3/4 columns), *NeuroD* (6/6), *Nscl2* (4/5), *Bhlhb5* (4/4), *NeuroD2* (4/4), *Math2* (5/5), *Tbr1* (4/5), and *VGlut2* (2/3) was observed after 24 h (Fig. 5G to N, Q, and R). However, even when massive VZ columns formed, *FezL* (0/1 column) and *Mef2c* (0/2) were not induced by *Ngn2* (Fig. 5O, P, and S), similar to their lack of induction by *Ngn2* ventrally. To further support the idea that *Ngn2* more efficiently induces the expression of downstream genes in dorsal versus ventral telencephalic domains, we also showed that approximately 27.5-fold more *Ngn2*-electroporated cells (EGFP positive) coexpressed the cortical marker Tbr1 in dorsal versus ventral telencephalic domains 48 h postelectroporation (Fig. 5T to V).

We conclude that *Ngn2* prematurely induces neurogenesis and the expression of a cortical transcriptional cascade in the dorsal telencephalon, acting at an accelerated rate compared to ventral domains, where many genes require 72 h for induction. We favor this interpretation over perturbed migration, as migration defects should result in *Ngn2*-induced cortical columns expressing all cortical markers, including *Mef2c* and *FezL*. Moreover, misexpression of *Ngn2* repressed *Pax6* expression in the cortical columns (see Fig. S6 in the supplemental material), as previously observed in the spinal cord (10), consistent with the idea that *Ngn2* has specific effects on gene expression.

Positioning *Math3* and *NeuroD* in the *Ngn2*-regulated genetic cascade. *Math3* and *NeuroD* are direct targets of *Ngn* genes in other systems (71). Consistent with similar genetic relationships existing in the cortex, both *Math3* and *NeuroD* were coexpressed to some extent with *Ngn2* (Fig. 1M to S) and are dependent on *Ngn2* for their transcription (see Fig. S1 in the supplemental material) (62). To determine if *Math3* and/or *NeuroD* are downstream effectors of *Ngn2* in the cortex, we compared their abilities to induce ectopic dorsal gene expression in the GE (see Table S2 in the supplemental material). Within 24 h postelectroporation at E12.5, *NeuroD* induced the ectopic expression of *Nscl2* (5/5 brains), *NeuroD2* (3/5), and *Math2* (2/5) in the GE (Fig. 6E to G), transcripts that remained detectable after 48 h, at which time *Tbr1* (3/6; not shown) and *VGlut2* (3/4; not shown) transcripts were also detected. Notably, *NeuroD* did not induce *Ngn2* expression in the GE (0/5 after 24 h) (Fig. 6B). Instead, *Ngn2* expression was suppressed by *NeuroD* in dorsal domains (see Fig. S6 in the supplemental material). However, in striking contrast to *Ngn2*, *NeuroD* induced ectopic *Math3* expression in the E12.5 GE at 24 h postelectroporation (3/5) (Fig. 6C), albeit in a transient manner (0/6 brains after 48 h). *NeuroD* is thus sufficient to induce ectopic cortical gene expression in the GE, acting at an accel-
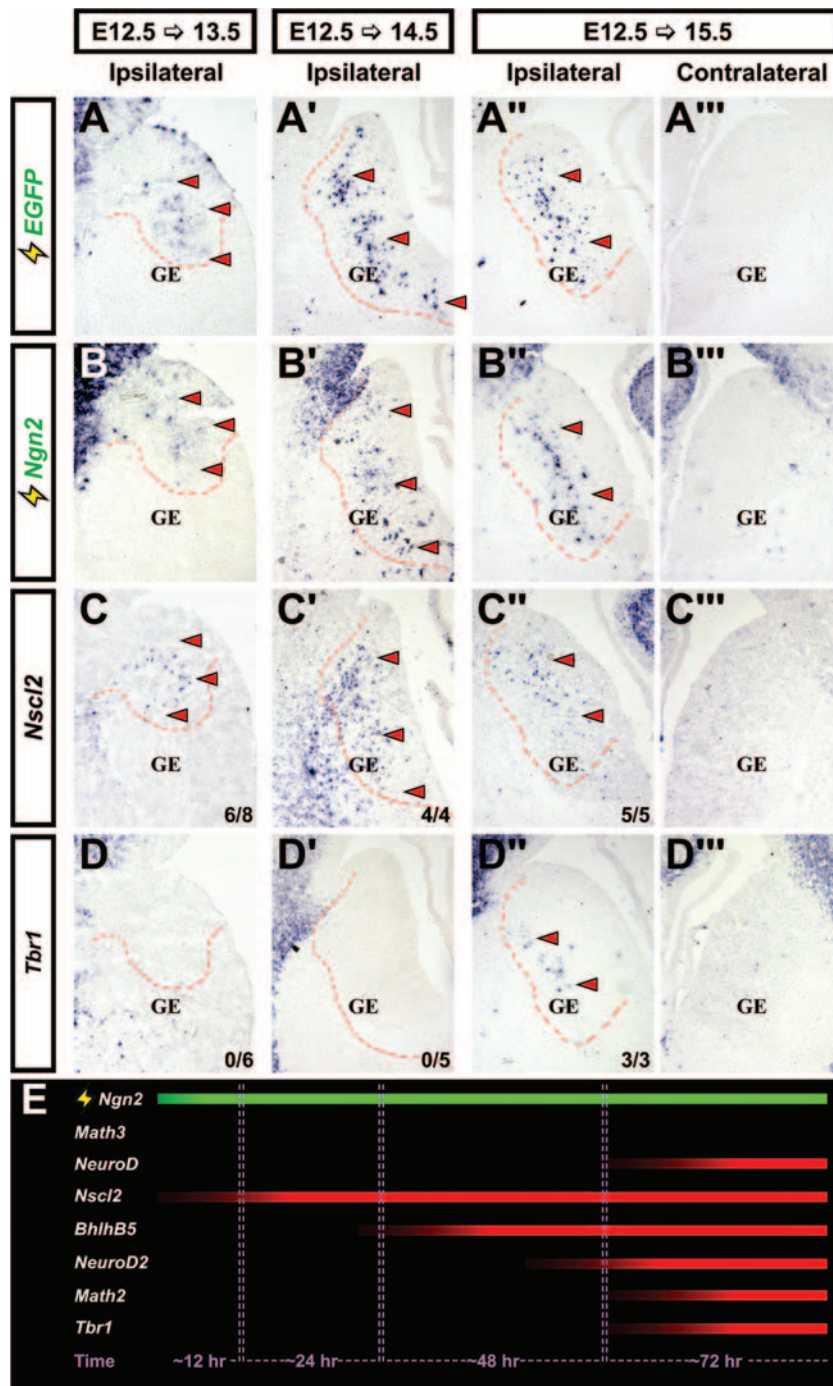
FIG. 4. Kinetics of ventral telencephalic gene induction downstream of *Ngn2*. Frontal sections of ventral telencephalons were electroporated at E12.5 with pCIG2-*Ngn2* and harvested at E13.5 (A to D), E14.5 (A′ to D′), or E15.5 (A″ to D″). Untransfected E15.5 telencephalons (contralateral) are shown in panels A‴ to D‴. Expression of the *EGFP*, *Ngn2*, *Nscl2*, and *Tbr1* genes (identified along the left side of the figure) is also shown. Dashed outlines indicate the approximate location of transfected cells. In panels C, C′, C″, D, D′, and D″, the numbers of times depicted results were observed are also indicated (lower-right corners). Arrowheads indicate ectopic transcripts. (E) Schematic illustrating the kinetics of gene induction downstream of *Ngn2* in the ventral telencephalon (continuous expression; green bar), showing approximate time required for detectable levels of each transcript to accumulate.

erated rate compared to *Ngn2* and in a *Ngn2*-independent fashion, suggesting that *NeuroD* acts downstream of *Ngn2* in the cortex. In contrast, in *Math3*-electroporated E12.5 GE analyzed after 24 h, ectopic expression of *Nscl2* (2/2) but not

Ngn2 (0/3) or *NeuroD* (0/3; not shown) was observed (see Table S3 in the supplemental material). After 48 h, *Math3*-electroporated GE cells continued to express *Nscl2* (7/7) and additionally expressed *BhlhB5* (5/8; not shown), *NeuroD2* (5/8),
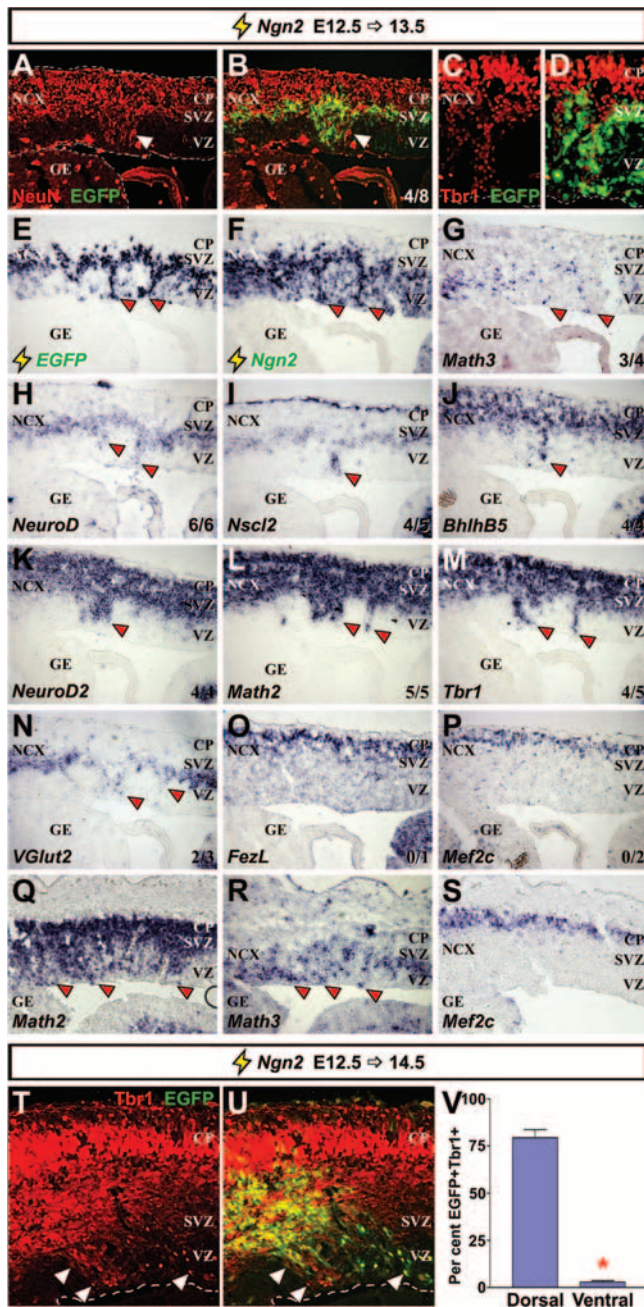
FIG. 5. *Ngn2* more rapidly induces cortical gene expression in the dorsal telencephalon. Frontal sections of cortices were electroporated at E12.5 with pCIG2-*Ngn2* and harvested at E13.5. (A to D) Visualization of EGFP epifluorescence (green; B and D) and immunolabeling for NeuN (red; A and B) or Tbr1 (red; C and D). (E to S) Localization of transcripts for *EGFP, Ngn2, Math3, NeuroD, Nscl2, BhlhB5, NeuroD2, Math2, Tbr1, VGlut2, FezL,* and *Mef2c* genes (identified on the panels). Panels Q to S show a more strongly transfected brain. The number of times each marker was ectopically expressed in cortical columns is indicated in panels B and G to P (lower-right corners). (T and U) Visualization of EGFP epifluorescence (green; T and U) and immunolabeling for Tbr1 (red; T and U) in the cortex. Arrowheads indicate ectopic transcript or protein expression. (V) Quantitation of EGFP/Tbr1 double-positive cells in dorsal and ventral transfections. The asterisk in panel V indicates a significant difference with a *P* value of <0.0001 (two-tailed *t* test). NCX, neocortex; CP, cortical plate.

and *Math2* (5/7) but not *NeuroD* (0/8) or *Tbr1* (0/8) (Fig. 6L to P), which were not detected until 72 h posttransfection. The rate of *Math3*-induced cortical gene transcription in the GE was thus intermediate between *Ngn2* and *NeuroD*.

We were struck by several differences in *Ngn2* function in dorsal versus ventral telencephalic domains. Firstly, *Ngn2* induced cortical gene expression at an accelerated rate in dorsal compared to ventral domains. Secondly, while premature *Math3* expression was induced by *Ngn2* in the dorsal telencephalon, *Math3* was not induced in the GE at any stage analyzed (6 to 96 h postelectroporation) (see Table S1 in the supplemental material). Finally, *NeuroD* was an early target of *Ngn2* in dorsal transfections but was a relatively late target in the GE. In skeletal muscle, the bHLH gene *MyoD* induces the expression of late target genes through cooperative interactions with *Myog*, another bHLH gene that functions later in the differentiation process (13). We therefore hypothesized that *Ngn2* could cooperate with *Math3* to more efficiently induce the expression of later-onset cortical genes (e.g., *NeuroD*). In this scenario, the absence of *Math3* induction by *Ngn2* in ventral domains might explain the differences in the kinetics of *Ngn2*-mediated gene induction in the ventral versus dorsal telencephalon.

To test if *Math3* cooperates with *Ngn2*, equivalent concentrations of each expression construct were coelectroporated in the E12.5 GE (1.5 μg/μl each, with a final concentration of 3 μg/μl, which is the same as the final concentration of DNA used for all single-construct transfections). While *Nscl2* was the only gene ectopically induced by a coexpression of both *Math3* and *Ngn2* in the GE within 24 h (see Table S4 in the supplemental material), after 48 h, *Math2* (5/5) and *NeuroD2* (5/5) transcripts were readily detected in 100% of electroporated GE (Fig. 6V and W), greater than the 62.5% (5/8) and 20% (1/5) of *Math3* and *Ngn2* single electroporations, respectively, in which these cortical genes were induced (see Tables S1 and S3 in the supplemental material). Moreover, *NeuroD* (4/4) and *Tbr1* (4/5) transcripts were induced within 48 h in GE transfected with *Math3* plus *Ngn2*; these transcripts were never observed in this time frame when *Math3* or *Ngn2* was transfected individually (Fig. 6T and X). Accordingly, when transfected GE sections were stained for Tbr1 protein after 48 h (Fig. 6Z to H'), fewer than 3% of EGFP-positive cells expressed Tbr1 in individual *Ngn2* or *Math3* transfections. However, the percentage of EGFP-positive cells that coexpressed Tbr1 after coexpression of *Ngn2* and *Math3* was significantly increased to nearly 10% (Fig. 6I'). *Ngn2* and *Math3* thus cooperate to accelerate cortical gene induction in the GE (Fig. 6Y).

Cooperative transcriptional interactions between *Math3* and *Ngn2*. To quantitate transcriptional cooperativity between *Ngn2* and *Math3*, we developed an in vivo luciferase assay using a *Ngn*-dependent *NeuroD* promoter to drive *luciferase* expression (30) and controlling for transfection efficiency with a β-*actin-lacZ* reporter (17) (Fig. 7A). Equivalent amounts of both promoter constructs were mixed with combinations of pCIG2, pCIG2-*Ngn2*, and/or pCIG2-*Math3* (2 μg/μl total) and electroporated into the E12.5 telencephalon, which was divided into dorsal and ventral domains 24 h postelectroporation (Fig. 7B, B', C, and C'). Luciferase and β-galactosidase activities were assayed in cortical and GE lysates, using β-galactosidase to normalize for transfection efficiency (Fig. 7D). Since *NeuroD* is not endogenously expressed in the ventral telencepha-
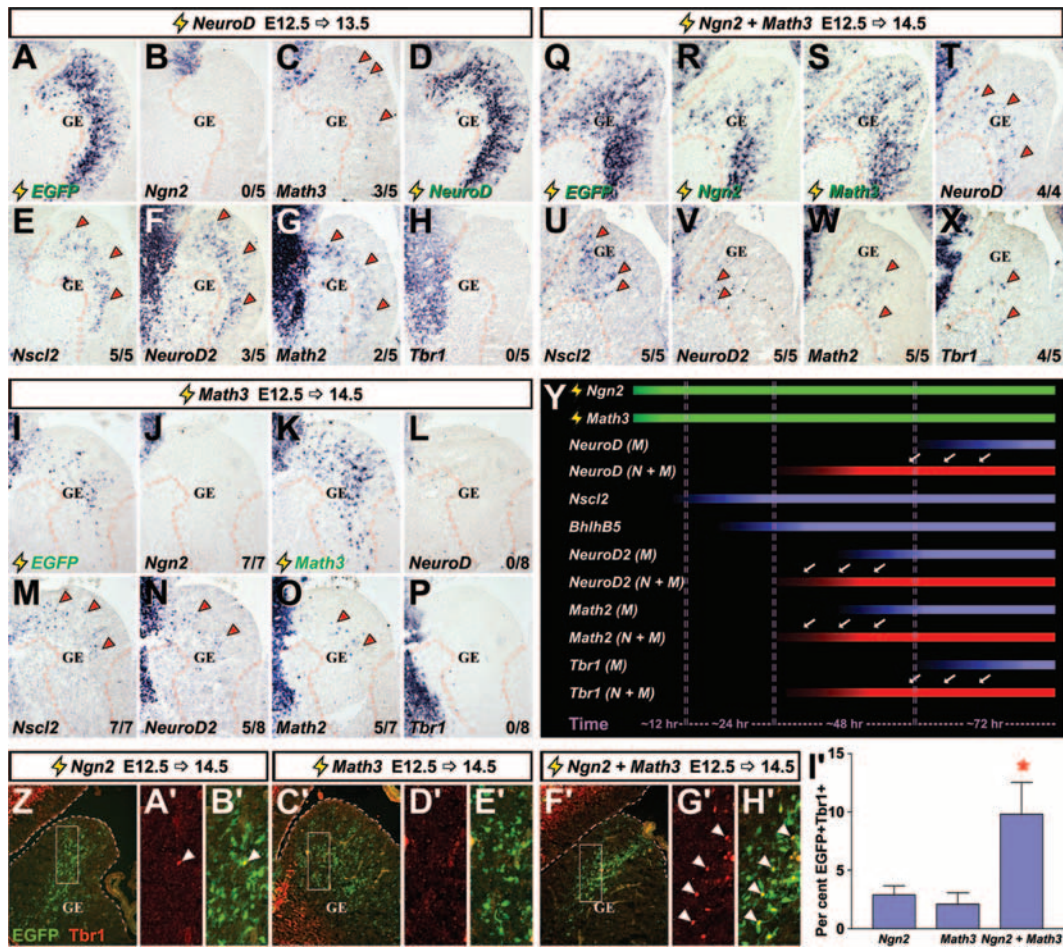
FIG. 6. Comparing the kinetics of cortical gene induction downstream of *NeuroD*, *Math3*, and *Ngn2* plus *Math3* in the ventral telencephalon. (A to H) Frontal sections of brains electroporated at E12.5 with pCIG2-*NeuroD* (3 μg/μl) and harvested at E13.5. (I to P) Frontal sections of brains electroporated at E12.5 with pCIG2-*Math3* (3 μg/μl) and harvested at E14.5. (Q to X) Frontal sections of brains electroporated at E12.5 with pCIG2-*Ngn2* and pCIG2-*Math3* (1.5 μg/μl each) and harvested at E14.5. Localizations of the transcripts are shown for the *EGFP*, *Ngn2*, *Math3*, *NeuroD*, *Nscl2*, *NeuroD2*, *Math2*, and *Tbr1* genes (identified on the panels). Arrowheads in panels A to X indicate ectopic expression. (Y) Schematic depicting shifts in the kinetics of gene induction when *Ngn2* and *Math3* are expressed together (*N*+*M*) versus *Math3* expressed alone (*M*). Green bars depict overexpressed genes, red bars depict genes with accelerated kinetics of induction when *Ngn2* and *Math3* are coexpressed (shift highlighted by arrows), and blue bars show gene expression induced by *Math3* alone. (Z to H′) Frontal sections of brains electroporated at E12.5 with pCIG2-*Ngn2* (3 μg/μl), pCIG2-*Math3* (3 μg/μl), and pCIG2-*Ngn2* plus pCIG2-*Math3* (1.5 μg/μl each) harvested at E14.5 (genes are identified above the panels). White boxes in Z, C′, and F′ indicate the positions of higher magnification images displayed shown in panels A′, B′, D′, E′, G′, and H′). Sections were stained with Tbr1 (red; arrowheads indicate double-positive cells). (I′) The percentage of EGFP-positive cells that expressed Tbr1. ∗, significantly different versus *Ngn2* ($P < 0.05$) and significantly different versus *Math3* ($P < 0.01$).

lon, *NeuroD* promoter activity in the ventral telencephalon was arbitrarily assigned a value of 1, against which all other values were normalized. As expected, basal *NeuroD* promoter activity was higher in dorsal (6.85 ± 1.50; $n = 21$) than ventral (1.00 ± 0.07; $n = 17$) domains ($P < 0.0001$) (Fig. 7E). Cotransfection of *Ngn2* did not further increase *NeuroD* promoter activity dorsally (5.28 ± 0.73; $n = 8$), ostensibly due to high levels of endogenous *Ngn2* (Fig. 7E). In contrast, in the ventral telencephalon, *Ngn2* increased *NeuroD* promoter activity approximately fourfold (1 μg/μl *Ngn2*, 4.11 ± 1.31 [$n = 7$; $P = 0.0133$]; 2 μg/μl *Ngn2*, 4.25 ± 0.53 [$n = 8$; $P < 0.0001$]), albeit only to ~60% of the activity levels observed dorsally ($P = 0.0076$ for pCIG2 dorsal versus twice the amount of *Ngn2*). *Math3* similarly had little effect on the *NeuroD* promoter in the dorsal telencephalon (1 μg/μl, 6.28 ± 0.73; $n = 8$) but efficiently

induced *NeuroD* promoter activity in ventral domains (1 μg/μl, 3.84 ± 0.39; $n = 10$; $P = 0.0002$ versus pCIG2 ventral) (Fig. 7E). In contrast, coexpression of *Ngn2* and *Math3* increased promoter drive ~1.4-fold in ventral (1 μg/μl each, 6.01 ± 0.82; $n = 12$; $P = 0.014$) domains, compared to equivalent amounts of *Ngn2* alone. Importantly, comparisons were made between the luciferase values obtained following electroporations of 2 μg/μl of *Ngn2* versus 1 μg/μl each of the coexpressed *Ngn2* and *Math3* (2 μg/μl together), such that the total amounts of bHLH DNA transfected were equivalent. We thus concluded that cotransfection of *Ngn2* and *Math3* synergizes on the *NeuroD* promoter in vivo, since additive interactions should have alternatively yielded equivalent activation levels in single and double electroporations.

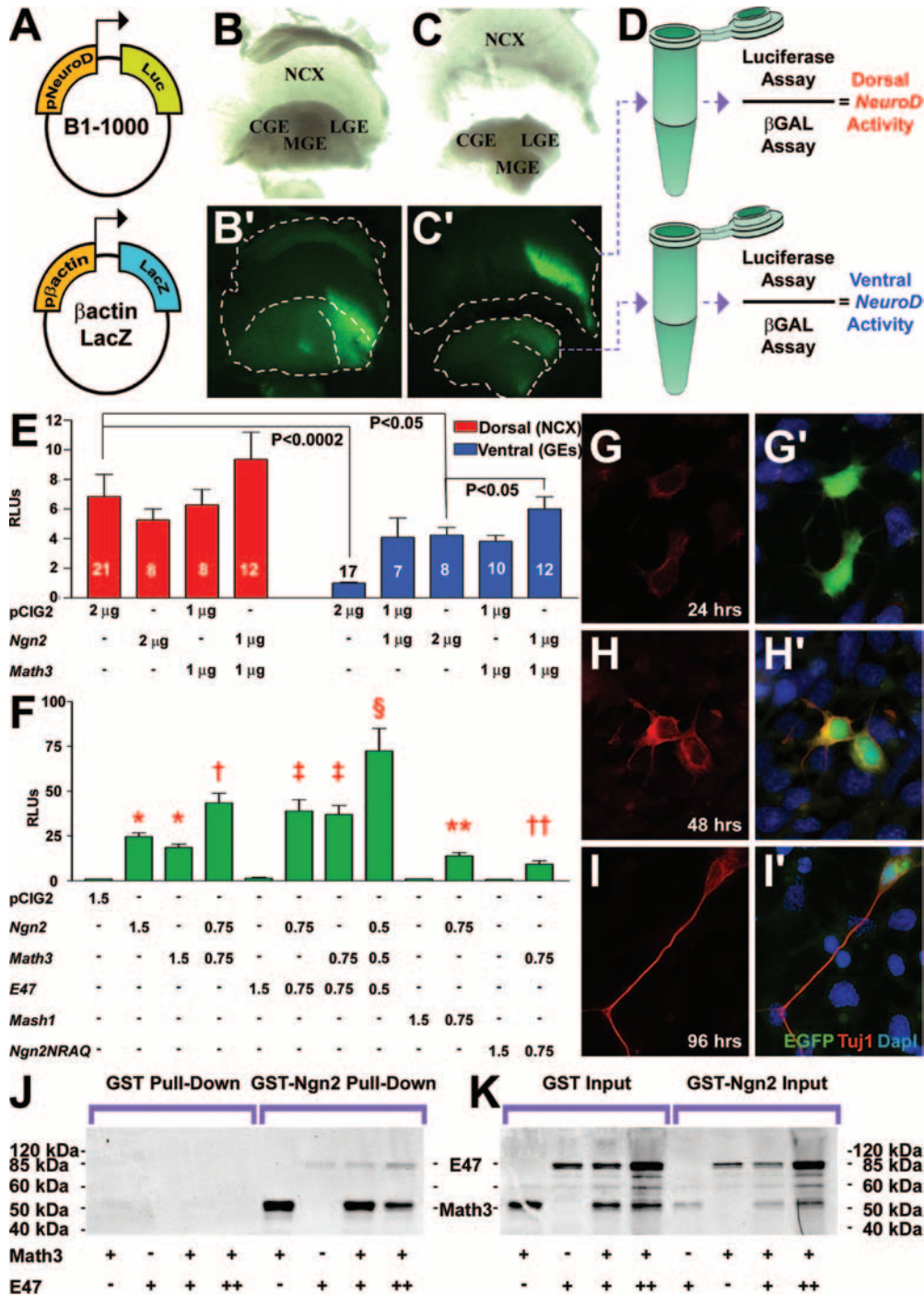To investigate further the synergism of the combination of

FIG. 7. *Ngn2* and *Math3* synergize on the *NeuroD* promoter. (A to E) In vivo luciferase assay. *NeuroD-luciferase* (A) and β-*actin-lacZ* (B) (1 μg/μl each) promoter constructs were combined with 2 μg/μl of pCIG2 combinations (pCIG2, *Ngn2* and/or *Math3*; shown in E) and electroporated into E12.5 telencephalons. Bright-field (B and C) and dark-field (B′ and C′) images are shown of an electroporated telencephalic vesicle harvested after 24 h (B and B′) and dissected into dorsal and ventral halves (C and C′), which were then measured for luciferase and β-galactosidase activity (D). (E) Normalized luciferase activity levels, showing relative induction when *NeuroD* promoter was expressed with various pCIG2 constructs. (F) Luciferase experiment in P19 cells, showing normalized luciferase levels with a *NeuroD* promoter construct cotransfected with various expression vectors. *, significantly different versus pCIG2 ($P < 0.01$); †, significantly different versus pCIG2, *Ngn2*, and *Math3* ($P < 0.001$); ‡, significantly different versus pCIG2 or *E47* ($P < 0.01$) and not significantly different versus *Ngn2* plus *Math3*; §, significantly different versus all other means ($P < 0.001$); **, significantly different versus pCIG2, *Ngn2*, and *Mash1* ($P < 0.001$); ††, significantly different versus pCIG2, *Ngn2*, *Math3*, and *Ngn2NRAQ* ($P < 0.05$). (G to I and G′ to I′) P19 cells transfected with *Ngn2* (green) expressed *Tuj1* (red) 48 h posttransfection. Blue is DAPI counterstain. (J and K) GST pull-down experiments with GST or GST-tagged Ngn2 protein immobilized on glutathione beads and combined with ^{35}S-labeled Math3 and/or E47, showing bound protein (J) and input protein (K). RLU, relative light units; NCX, neocortex; LGE, lateral ganglionic eminence; MGE, medial ganglionic eminence; CGE, caudal ganglionic eminence; Luc, luciferase; β-Gal, β-galactosidase.
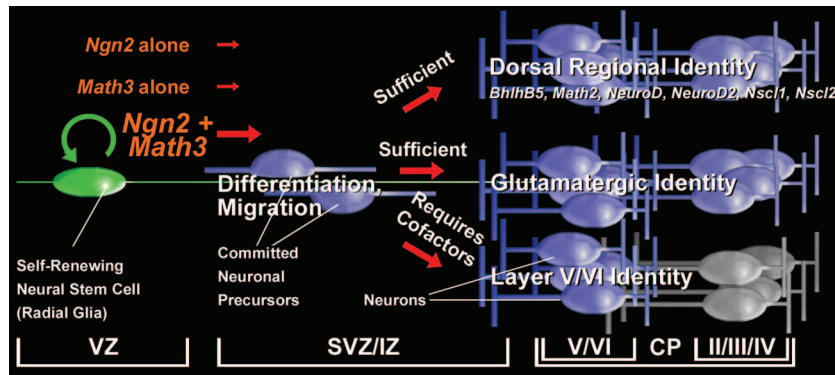
FIG. 8. Model of *Ngn2* genetic cascades in the cortex. *Ngn2*, which is expressed in cycling cortical progenitors, initiates neuronal differentiation and specifies aspects of a neocortical projection neuron identity including neurotransmitter and regional identities. *Ngn2* can induce *Math3* expression in the dorsal telencephalon but requires context-specific cofactors which are not present in the ventral telencephalon to do so. The instructive power of *Ngn2* does not extend to all cortical marker genes nor to lamina-specific genes, which must be activated by independent or codependent genetic pathways. CP, cortical plate; IZ, intermediate zone.

Ngn2 and *Math3*, we used P19 embryonal carcinoma cells, which differentiate into neurons in response to bHLH genes (18) (Fig. 7G to I and G′ to I′). P19 cells were transfected with equivalent amounts of the *NeuroD* and β-galactosidase promoter constructs and 1.5 μg/μl total of pCIG2 expression vectors (four independent experiments, with 12 replicates for each set of constructs) (Fig. 7F). While *Ngn2* and *Math3* transactivated the *NeuroD* promoter when transfected alone (pCIG2, 1.00 ± 0.01; *Ngn2*, 24.76 ± 2.24; *Math3*, 18.67 ± 1.95; $P <$ 0.001 for *Ngn2* and $P <$ 0.01 for *Math3*, both versus pCIG2), cotransfection of *Math3* and *Ngn2* doubled *NeuroD* transactivation (43.52 ± 5.40; $P <$ 0.001 versus all other means). Proneural bHLH proteins are thought to form obligate heterodimers with E2A bHLH proteins (e.g., E47) but are also capable of promiscuous heterodimerization (22). Accordingly, while *E47* did not transactivate the *NeuroD* promoter by itself (1.67 ± 0.43), coexpression of *E47* with *Ngn2* or *Math3* yielded about a twofold increase in promoter drive (*Ngn2* plus *E47*, 39.05 ± 6.34; *Math3* plus *E47*, 37.01 ± 5.08) (Fig. 7F). Strikingly, when the three bHLH genes were coexpressed in equal ratios (0.5 μg/μl each) and with the same total amount of bHLH DNA (1.5 μg/μl), there was a further 1.66-fold boost in promoter activity (72.55 ± 12.51; $P <$ 0.001). The synergism between *Ngn2* and *Math3* was not generic to all bHLH genes as cotransfections of *Ngn2* and the bHLH gene *Mash1* (0.75 μg/μl each; 1.5 μg/μl total) resulted in activity levels that were roughly equivalent to transfecting a half-dosage of *Ngn2* (14.12 ± 1.70; $P <$ 0.001 versus 1.5 μg/μl *Ngn2*). Similarly, cotransfection of *Math3* with *Ngn2NRAQ*, a DNA-binding domain mutant (0.75 μg/μl each) reduced transcriptional activity by half (9.35 ± 1.94) compared to double dosages (1.5 μg/μl) of *Math3* ($P <$ 0.01) or *Ngn2* ($P <$ 0.001). The DNA binding activity of *Ngn2* is thus obligatory for cooperation with *Math3*.

To test if Ngn2 and Math3 proteins formed direct physical interactions, we performed GST pull-down assays. In vitro transcribed and translated, ^{35}S-labeled Math3 efficiently bound immobilized GST-tagged Ngn2 but not GST alone (Fig. 7J). To test the effects of E47 on Ngn2-Math3 heterodimer formation, equivalent amounts of ^{35}S-Math3 were mixed with increasing amounts of ^{35}S-E47 (Fig. 7K, inputs) and then incubated with GST and GST-Ngn2-bound beads. Although E47 bound poorly to GST-Ngn2 relative to Math3, doubling the amount of E47 competitor reduced the amount of Math3 bound by approximately half (a 56% reduction in input-normalized optical density; normalized Math3 values were 255.7 with the initial amount of E47 and 113.2 with twice the amount of E47) (Fig. 7J). This strongly suggests that Math3 and E47 compete for the same binding site in Ngn2, likely the HLH domain.

DISCUSSION

Neuronal differentiation occurs in a series of interdependent steps that require the strict temporal and spatial coordination of gene expression. In the cortex, several genes have been identified that participate in the specification of a glutamatergic projection neuron identity, yet few studies have examined how these genes are organized into genetic networks or conclusively determined if they are instructive or permissive determinants of neuronal identity. We report here that *Ngn2* acts instructively to promote a cortical neuronal identity in the ventral telencephalon, inducing cortical gene expression in a defined temporal order. Surprisingly, however, for *Ngn2* to efficiently and rapidly promote the expression of cortical genes, it must cooperate with a second bHLH gene, *Math3*, with which it forms physical interactions. Our study thus provides an important framework for understanding how bHLH genes cooperate to determine aspects of neuronal subtype identity in the cortex (Fig. 8).

***Ngn2* instructively induces the expression of a network of cortical genes.** The early expression of *Ngn2* in VZ progenitors was consistent with its acting at the top of a cortical transcriptional cascade. Indeed, misexpression of *Ngn2* in ventral telencephalic progenitors was sufficient to induce the ectopic expression of several cortical genes, including markers of a dorsal regional and glutamatergic neuronal identity. However, *Ngn2* was not sufficient to induce expression of all cortical markers (e.g., *FezL* and *Mef2c*), including layer-specific genes, suggesting that it promotes a partial cortical identity. Nevertheless, this is one of the first examples in the central nervous

system where a *Ngn* gene is instructive for neuronal subtype identity. For instance, in the spinal cord, *Ngn2* is not sufficient to promote motoneuron or other ventral neuronal identities (45, 53, 55). Instead, *Ngn2* mediates generic neuronal differentiation in motor neuron progenitors, an activity that is temporally coordinated with fate specification via interactions with the LIM homeodomain transcription factors *Lhx3* and *Islet1* (38). *Ngn1* and *Ngn2* also mediate generic neuronal differentiation and not cell fate specification in other contexts, such as the midbrain (32). In contrast, in the peripheral nervous system, *Ngn1* and *Ngn2* act instructively in neural crest cells to promote a sensory neuron identity, albeit in a context-dependent fashion (41, 54).

While at first glance our results conflict with a previous study in which *Ngn2* was knocked into the *Mash1* locus and was not sufficient to respecify ventral telencephalic progenitors (53), there are several key differences in the two studies. With the approach used herein, *Ngn2* was expressed from a strong cytomegalovirus/β-actin enhancer/promoter that leads to high and protracted expression. This contrasts to the genetic approach, where *Ngn2* was ectopically expressed in ventral telencephalic progenitors under the control of *Mash1* regulatory sequences, leading to transient and more physiological expression levels (53). While the ability of *Ngn2* to promote a cortical identity may be an artifact of the superphysiological levels of expression obtained by in utero electroporation, the ability of exogenous *Ngn2* to transactivate the *NeuroD* promoter was considerably lower in the ventral telencephalon than the transactivation achieved with endogenous *Ngn2* in cortical progenitors. Moreover, the initiation of cortical marker expression by *Ngn2* took up to three times longer in the ventral telencephalon. We thus favor the interpretation that sustained expression (rather than overexpression) of *Ngn2* is the critical difference in these two approaches. According to this model, *Ngn2* would require a dorsally restricted cofactor(s) in order to achieve the rapid gene induction kinetics observed in the dorsal telencephalon. In its absence, *Ngn2* would require more time to trigger gene expression (which does not occur in the knock-in model), either because its transactivation strength is subthreshold or because of additional mechanisms that repress target gene transcription in ventral domains (e.g., epigenetic modifications).

Synergistic interactions between *Ngn2* and *Math3*. Several observations suggested that *Math3* is an essential cofactor that is required for *Ngn2* to promote a cortical fate efficiently. First, *Math3* is dorsally restricted and highly coexpressed with *Ngn2* in cortical progenitors. Second, *Math3* expression is lost (or sharply downregulated) in *Ngn2* mutant cortices, suggesting that the loss of this gene may contribute to the downregulation of cortical gene expression observed in *Ngn2* mutants. The future analysis of *Math3* single mutants will be informative in this regard. Third, in ventral domains where *Ngn2* activity is sharply attenuated, *Math3* is not induced by ectopic *Ngn2*. This was surprising, as *Math3* is a transcriptional target of *Ngn* in the spinal cord and *Xenopus* ectoderm (55, 71). However, in *Ngn2* mutant retina, *Math3* expression instead increases (1), suggesting that genetic interactions between *Ngn2* and *Math3* are context dependent. Fourth, *Math3* activates the same transcriptional targets as *Ngn2* in the ventral telencephalon, displaying similar, albeit slightly faster kinetics. Consistent with

our model of cooperativity, coexpression of *Math3* and *Ngn2* in the ventral telencephalon boosted *NeuroD* promoter activity ~1.4-fold, achieving transcriptional activation levels approaching those observed in the cortex in the absence of exogenous bHLH expression. Moreover, the observed boost in promoter drive correlated with the faster onset of target gene expression when *Ngn2* and *Math3* are coexpressed.

The mechanism(s) responsible for the observed cooperativity between *Ngn2* and *Math3* remains to be fully elucidated. One possibility is that Ngn2 and Math3, which, we showed, physically interact, might act as a heterodimer to activate target genes. Furthermore, our data suggest that while E47 can compete for the interaction domains of Ngn2 and Math3, it enhances functional cooperation between Ngn2 and Math3 rather than acting as a competitor. One possibility is that Ngn2, Math3, and E2A proteins generate a variety of heterodimer combinations. Ngn2/E47 and Math3/E47 heterodimers could act independently by binding to distinct promoter/enhancer elements or by recruiting different cofactors to modulate promoter architecture, as has been proposed for the myogenic bHLH genes *MyoD* and *MyoG* (13).

The nested expression of bHLH genes in progenitors and more differentiated cell types has been observed in neural and nonneural tissues. This has traditionally been interpreted to indicate that these genes act sequentially, first to determine and then to differentiate cells (11, 58). Although the bHLH genes *Ngn2* and *Math3* were thought to act in a linear sequence, we showed here that they cooperate to activate downstream gene expression. Yet we have also shown that *Math3* or *Ngn2* can also act independently to initiate gene expression, albeit with a temporal delay. Our data thus help explain why deleting a single bHLH gene often fails to yield a phenotype, except where very rapid and/or precisely timed differentiation events are required.

REFERENCES

1. **Akagi, T., T. Inoue, G. Miyoshi, Y. Bessho, M. Takahashi, J. E. Lee, F. Guillemot, and R. Kageyama.** 2004. Requirement of multiple basic helix-loop-helix genes for retinal neuronal subtype specification. J. Biol. Chem. **279:**28492–28498.
2. **Alam, S., D. Zinyk, L. Ma, and C. Schuurmans.** 2005. Members of the Plag gene family are expressed in complementary and overlapping regions in the developing murine nervous system. Dev. Dyn. **234:**772–782.
3. **Anselmo, M. A., S. Dalvin, P. Prodhan, K. Komatsuzaki, J. T. Aidlen, J. J. Schnitzer, J. Y. Wu, and T. B. Kinane.** 2003. Slit and robo: expression patterns in lung development. Gene Expr. Patterns **3:**13–19.
4. **Arai, Y., N. Funatsu, K. Numayama-Tsuruta, T. Nomura, S. Nakamura, and N. Osumi.** 2005. Role of Fabp7, a downstream gene of Pax6, in the maintenance of neuroepithelial cells during early embryonic development of the rat cortex. J. Neurosci. **25:**9752–9761.

5. **Arber, S., D. R. Ladle, J. H. Lin, E. Frank, and T. M. Jessell.** 2000. ETS gene Er81 controls the formation of functional connections between group Ia sensory afferents and motor neurons. Cell **101:**485–498.

6. **Backman, M., O. Machon, L. Mygland, C. J. van den Bout, W. Zhong, M. M. Taketo, and S. Krauss.** 2005. Effects of canonical Wnt signaling on dorso-ventral specification of the mouse telencephalon. Dev. Biol. **279:**155–168.

7. **Bartholoma, A., and K. A. Nave.** 1994. NEX-1: a novel brain-specific helix-loop-helix protein with autoregulation and sustained expression in mature cortical neurons. Mech. Dev. **48:**217–228.

8. **Begley, C. G., S. Lipkowitz, V. Gobel, K. A. Mahon, V. Bertness, A. R. Green, N. M. Gough, and I. R. Kirsch.** 1992. Molecular characterization of NSCL, a gene encoding a helix-loop-helix protein expressed in the developing nervous system. Proc. Natl. Acad. Sci. USA **89:**38–42.

9. **Behar, T., W. Ma, L. Hudson, and J. L. Barker.** 1994. Analysis of the anatomical distribution of GAD67 mRNA encoding truncated glutamic acid decarboxylase proteins in the embryonic rat brain. Brain Res. Dev. Brain Res. **77:**77–87.

10. **Bel-Vialar, S., F. Medevielle, and F. Pituello.** 2007. The on/off of Pax6 controls the tempo of neuronal differentiation in the developing spinal cord. Dev. Biol. **305:**659–673.

11. **Bertrand, N., D. S. Castro, and F. Guillemot.** 2002. Proneural genes and the specification of neural cell types. Nat. Rev. Neurosci **3:**517–530.

12. **Britz, O., P. Mattar, L. Nguyen, L. M. Langevin, C. Zimmer, S. Alam, F. Guillemot, and C. Schuurmans.** 2006. A role for proneural genes in the maturation of cortical progenitor cells. Cereb. Cortex **16:**i138–i151.

13. **Cao, Y., R. M. Kumar, B. H. Penn, C. A. Berkes, C. Kooperberg, L. A. Boyer, R. A. Young, and S. J. Tapscott.** 2006. Global and gene-specific analyses show distinct roles for Myod and Myog at a common set of promoters. EMBO J. **25:**502–511.

14. **Cau, E., S. Casarosa, and F. Guillemot.** 2002. Mash1 and Ngn1 control distinct steps of determination and differentiation in the olfactory sensory neuron lineage. Development **129:**1871–1880.

15. **Chen, B., L. R. Schaevitz, and S. K. McConnell.** 2005. Fezl regulates the differentiation and axon targeting of layer 5 subcortical projection neurons in cerebral cortex. Proc. Natl. Acad. Sci. **102:**17184–17189.

16. **Cheng, L., A. Arata, R. Mizuguchi, Y. Qian, A. Karunaratne, P. A. Gray, S. Arata, S. Shirasawa, M. Bouchard, P. Luo, C. L. Chen, M. Busslinger, M. Goulding, H. Onimaru, and Q. Ma.** 2004. Tlx3 and Tlx1 are post-mitotic selector genes determining glutamatergic over GABAergic cell fates. Nat. Neurosci. **7:**510–517.

17. **Cross, J. C., M. L. Flannery, M. A. Blanar, E. Steingrimsson, N. A. Jenkins, N. G. Copeland, W. J. Rutler, and Z. Werb.** 1995. Hxt encodes a basic helix-loop-helix transcription factor that regulates trophoblast cell development. Development **121:**2513–2523.

18. **Farah, M. H., J. M. Olson, H. B. Sucic, R. I. Hume, S. J. Tapscott, and D. L. Turner.** 2000. Generation of neurons by transient expression of neural bHLH proteins in mammalian cells. Development **127:**693–702.

19. **Fode, C., Q. Ma, S. Casarosa, S. L. Ang, D. J. Anderson, and F. Guillemot.** 2000. A role for neural determination genes in specifying the dorsoventral identity of telencephalic neurons. Genes Dev. **14:**67–80.

20. **Fremeau, R. T., Jr., M. D. Troyer, I. Pahner, G. O. Nygaard, C. H. Tran, R. J. Reimer, E. E. Bellocchio, D. Fortin, J. Storm-Mathisen, and R. H. Edwards.** 2001. The expression of vesicular glutamate transporters defines two classes of excitatory synapse. Neuron **31:**247–260.

21. **Ge, W., F. He, K. J. Kim, B. Blanchi, V. Coskun, L. Nguyen, X. Wu, J. Zhao, J. I. Heng, K. Martinowich, J. Tao, H. Wu, D. Castro, M. M. Sobeih, G. Corfas, J. G. Gleeson, M. E. Greenberg, F. Guillemot, and Y. E. Sun.** 2006. Coupling of cell migration with neurogenesis by proneural bHLH factors. Proc. Natl. Acad. Sci. USA **103:**1319–1324.

22. **Gradwohl, G., C. Fode, and F. Guillemot.** 1996. Restricted expression of a novel murine atonal-related bHLH protein in undifferentiated neural precursors. Dev. Biol. **180:**227–241.

23. **Guillemot, F., and A. L. Joyner.** 1993. Dynamic expression of the murine Achaete-Scute homologue Mash-1 in the developing nervous system. Mech. Dev. **42:**171–185.

24. **Gunhaga, L., M. Marklund, M. Sjodal, J. C. Hsieh, T. M. Jessell, and T. Edlund.** 2003. Specification of dorsal telencephalic character by sequential Wnt and FGF signaling. Nat. Neurosci. **6:**701–707.

25. **Gunnersen, J. M., C. Augustine, V. Spirkoska, M. Kim, M. Brown, and S. S. Tan.** 2002. Global analysis of gene expression patterns in developing mouse neocortex using serial analysis of gene expression. Mol. Cell Neurosci. **19:**560–573.

26. **Hand, R., D. Bortone, P. Mattar, L. Nguyen, J. I. Heng, S. Guerrier, E. Boutt, E. Peters, A. P. Barnes, C. Parras, C. Schuurmans, F. Guillemot, and F. Polleux.** 2005. Phosphorylation of Neurogenin2 specifies the migration properties and the dendritic morphology of pyramidal neurons in the neocortex. Neuron **48:**45–62.

27. **Hevner, R. F., L. Shi, N. Justice, Y. Hsueh, M. Sheng, S. Smiga, A. Bulfone, A. M. Goffinet, A. T. Campagnoni, and J. L. Rubenstein.** 2001. Tbr1 regulates differentiation of the preplate and layer 6. Neuron **29:**353–366.

28. **Hirata, T., Y. Suda, K. Nakao, M. Narimatsu, T. Hirano, and M. Hibi.** 2004.

29. **Holm, P. C., M. T. Mader, N. Haubst, A. Wizenmann, M. Sigvardsson, and M. Gotz.** 2007. Loss- and gain-of-function analyses reveal targets of Pax6 in the developing mouse telencephalon. Mol. Cell Neurosci. **34:**99–119.

30. **Huang, H. P., M. Liu, H. M. El-Hodiri, K. Chu, M. Jamrich, and M. J. Tsai.** 2000. Regulation of the pancreatic islet-specific gene *BETA2* (*neuroD*) by neurogenin 3. Mol. Cell. Biol. **20:**3292–3307.

31. **Jeong, J. Y., Z. Einhorn, S. Mercurio, S. Lee, B. Lau, M. Mione, S. W. Wilson, and S. Guo.** 2006. Neurogenin1 is a determinant of zebrafish basal forebrain dopaminergic neurons and is regulated by the conserved zinc finger protein Tof/Fezl. Proc. Natl. Acad. Sci. USA **103:**5143–5148.

32. **Kele, J., N. Simplicio, A. L. Ferri, H. Mira, F. Guillemot, E. Arenas, and S. L. Ang.** 2006. Neurogenin 2 is required for the development of ventral midbrain dopaminergic neurons. Development **133:**495–505.

33. **Kim, C. H., Y. K. Bae, Y. Yamanaka, S. Yamashita, T. Shimizu, R. Fujii, H. C. Park, S. Y. Yeo, T. L. Huh, M. Hibi, and T. Hirano.** 1997. Overexpression of neurogenin induces ectopic expression of HuC in zebrafish. Neurosci. Lett. **239:**113–116.

34. **Kruger, M., and T. Braun.** 2002. The neuronal basic helix-loop-helix transcription factor NSCL-1 is dispensable for normal neuronal development. Mol. Cell. Biol. **22:**792–800.

35. **Kruger, M., T. Schmid, S. Kruger, E. Bober, and T. Braun.** 2006. Functional redundancy of NSCL-1 and NeuroD during development of the petrosal and vestibulocochlear ganglia. Eur. J. Neurosci. **24:**1581–1590.

36. **Langevin, L. M., P. Mattar, R. Scardigli, M. Roussigne, C. Logan, P. Blader, and C. Schuurmans.** 2007. Validating in utero electroporation for the rapid analysis of gene regulatory elements in the murine telencephalon. Dev. Dyn. **236:**1273–1286.

37. **Lee, J. E., S. M. Hollenberg, L. Snider, D. L. Turner, N. Lipnick, and H. Weintraub.** 1995. Conversion of *Xenopus* ectoderm into neurons by NeuroD, a basic helix-loop-helix protein. Science **268:**836–844.

38. **Lee, S. K., and S. L. Pfaff.** 2003. Synchronization of neurogenesis and motor neuron specification by direct coupling of bHLH and homeodomain transcription factors. Neuron **38:**731–745.

39. **Lin, X., M. W. State, F. M. Vaccarino, J. Greally, M. Hass, and J. F. Leckman.** 1999. Identification, chromosomal assignment, and expression analysis of the human homeodomain-containing gene Orthopedia (OTP). Genomics **60:**96–104.

40. **Liu, M., S. J. Pleasure, A. E. Collins, J. L. Noebels, F. J. Naya, M. J. Tsai, and D. H. Lowenstein.** 2000. Loss of BETA2/NeuroD leads to malformation of the dentate gyrus and epilepsy. Proc. Natl. Acad. Sci. USA **97:**865–870.

41. **Lo, L., E. Dormand, A. Greenwood, and D. J. Anderson.** 2002. Comparison of the generic neuronal differentiation and neuron subtype specification functions of mammalian achaete-scute and atonal homologs in cultured neural progenitor cells. Development **129:**1553–1567.

42. **Machon, O., M. Backman, S. Krauss, and Z. Kozmik.** 2005. The cellular fate of cortical progenitors is not maintained in neurosphere cultures. Mol. Cell Neurosci. **30:**388–397.

43. **Martin, J. F., J. J. Schwarz, and E. N. Olson.** 1993. Myocyte enhancer factor (MEF) 2C: a tissue-restricted member of the MEF-2 family of transcription factors. Proc. Natl. Acad. Sci. USA **90:**5282–5286.

44. **Mattar, P., O. Britz, C. Johannes, M. Nieto, L. Ma, A. Rebeyka, N. Klenin, F. Polleux, F. Guillemot, and C. Schuurmans.** 2004. A screen for downstream effectors of Neurogenin2 in the embryonic neocortex. Dev. Biol. **273:**373–389.

45. **Mizuguchi, R., M. Sugimori, H. Takebayashi, H. Kosako, M. Nagao, S. Yoshida, Y. Nabeshima, K. Shimamura, and M. Nakafuku.** 2001. Combinatorial roles of olig2 and neurogenin2 in the coordinated induction of pan-neuronal and subtype-specific properties of motoneurons. Neuron **31:**757–771.

46. **Molyneaux, B. J., P. Arlotta, T. Hirata, M. Hibi, and J. D. Macklis.** 2005. Fezl is required for the birth and specification of corticospinal motor neurons. Neuron **47:**817–831.

47. **Molyneaux, B. J., P. Arlotta, J. R. Menezes, and J. D. Macklis.** 2007. Neuronal subtype specification in the cerebral cortex. Nat. Rev. Neurosci **8:**427–437.

48. **Monuki, E. S., F. D. Porter, and C. A. Walsh.** 2001. Patterning of the dorsal telencephalon and cerebral cortex by a roof plate-Lhx2 pathway. Neuron **32:**591–604.

49. **Muzio, L., B. DiBenedetto, A. Stoykova, E. Boncinelli, P. Gruss, and A. Mallamaci.** 2002. Conversion of cerebral cortex into basal ganglia in Emx2(−/−) Pax6(Sey/Sey) double-mutant mice. Nat. Neurosci. **5:**737–745.

50. **Nakatani, T., Y. Minaki, M. Kumai, and Y. Ono.** 2007. Helt determines GABAergic over glutamatergic neuronal fate by repressing Ngn genes in the developing mesencephalon. Development **134:**2783–2793.

51. **Olson, J. M., A. Asakura, L. Snider, R. Hawkes, A. Strand, J. Stoeck, A. Hallahan, J. Pritchard, and S. J. Tapscott.** 2001. NeuroD2 is necessary for development and survival of central nervous system neurons. Dev. Biol. **234:**174–187.

52. **Parker, M. H., P. Seale, and M. A. Rudnicki.** 2003. Looking back to the

Zinc finger gene fez-like functions in the formation of subplate neurons and thalamocortical axons. Dev. Dyn. **230:**546–556.

embryo: defining transcriptional networks in adult myogenesis. Nat. Rev. Genet. **4:**497–507.

53. **Parras, C. M., C. Schuurmans, R. Scardigli, J. Kim, D. J. Anderson, and F. Guillemot.** 2002. Divergent functions of the proneural genes Mash1 and Ngn2 in the specification of neuronal subtype identity. Genes Dev. **16:**324–338.

54. **Perez, S. E., S. Rebelo, and D. J. Anderson.** 1999. Early specification of sensory neuron fate revealed by expression and function of neurogenins in the chick embryo. Development **126:**1715–1728.

55. **Perron, M., K. Opdecamp, K. Butler, W. A. Harris, and E. J. Bellefroid.** 1999. X-ngnr-1 and Xath3 promote ectopic expression of sensory neuron markers in the neurula ectoderm and have distinct inducing properties in the retina. Proc. Natl. Acad. Sci. USA **96:**14996–15001.

56. **Puelles, E., D. Acampora, R. Gogoi, F. Tuorto, A. Papalia, F. Guillemot, S. L. Ang, and A. Simeone.** 2006. Otx2 controls identity and fate of glutamatergic progenitors of the thalamus by repressing GABAergic differentiation. J. Neurosci. **26:**5955–5964.

57. **Rash, B. G., and E. A. Grove.** 2006. Area and layer patterning in the developing cerebral cortex. Curr. Opin. Neurobiol. **16:**25–34.

58. **Ross, S. E., M. E. Greenberg, and C. D. Stiles.** 2003. Basic helix-loop-helix factors in cortical development. Neuron **39:**13–25.

59. **Saito, T., and N. Nakatsuji.** 2001. Efficient gene transfer into the embryonic mouse brain using in vivo electroporation. Dev. Biol. **240:**237–246.

60. **Scardigli, R., C. Schuurmans, G. Gradwohl, and F. Guillemot.** 2001. Cross-regulation between Neurogenin2 and pathways specifying neuronal identity in the spinal cord. Neuron **31:**203–217.

61. **Schaeren-Wiemers, N., E. Andre, J. P. Kapfhammer, and M. Becker-Andre.** 1997. The expression pattern of the orphan nuclear receptor RORbeta in the developing and adult rat nervous system suggests a role in the processing of sensory information and in circadian rhythm. Eur. J. Neurosci. **9:**2687–2701.

62. **Schuurmans, C., O. Armant, M. Nieto, J. M. Stenman, O. Britz, N. Klenin, C. Brown, L. M. Langevin, J. Seibt, H. Tang, J. M. Cunningham, R. Dyck, C. Walsh, K. Campbell, F. Polleux, and F. Guillemot.** 2004. Sequential phases of cortical specification involve Neurogenin-dependent and -independent pathways. EMBO J. **23:**2892–2902.

63. **Schuurmans, C., and F. Guillemot.** 2002. Molecular mechanisms underlying cell fate specification in the developing telencephalon. Curr. Opin. Neurobiol. **12:**26–34.

64. **Schwab, M. H., A. Bartholomae, B. Heimrich, D. Feldmeyer, S. Druffel-Augustin, S. Goebbels, F. J. Naya, S. Zhao, M. Frotscher, M. J. Tsai, and K. A. Nave.** 2000. Neuronal basic helix-loop-helix proteins (NEX and BETA2/Neuro D) regulate terminal granule cell differentiation in the hippocampus. J. Neurosci. **20:**3714–3724.

65. **Schwab, M. H., S. Druffel-Augustin, P. Gass, M. Jung, M. Klugmann, A.**

Bartholomae, M. J. Rossner, and K. A. Nave. 1998. Neuronal basic helix-loop-helix proteins (NEX, neuroD, NDRF): spatiotemporal expression and targeted disruption of the NEX gene in transgenic mice. J. Neurosci. **18:**1408–1418.

66. **Seo, S., J. W. Lim, D. Yellajoshyula, L. W. Chang, and K. L. Kroll.** 2007. Neurogenin and NeuroD direct transcriptional targets and their regulatory enhancers. EMBO J. **26:**5093–5108.

67. **Simmons, D. G., A. L. Fortier, and J. C. Cross.** 2007. Diverse subtypes and developmental origins of trophoblast giant cells in the mouse placenta. Dev. Biol. **304:**567–578.

68. **Stenman, J., R. T. Yu, R. M. Evans, and K. Campbell.** 2003. Tlx and Pax6 co-operate genetically to establish the pallio-subpallial boundary in the embryonic mouse telencephalon. Development **130:**1113–1122.

69. **Sun, Y., M. Nadal-Vicens, S. Misono, M. Z. Lin, A. Zubiaga, X. Hua, G. Fan, and M. E. Greenberg.** 2001. Neurogenin promotes neurogenesis and inhibits glial differentiation by independent mechanisms. Cell **104:**365–376.

70. **Takebayashi, K., S. Takahashi, C. Yokota, H. Tsuda, S. Nakanishi, M. Asashima, and R. Kageyama.** 1997. Conversion of ectoderm into a neural fate by ATH-3, a vertebrate basic helix-loop-helix gene homologous to *Drosophila* proneural gene atonal. EMBO J. **16:**384–395.

71. **Talikka, M., S. E. Perez, and K. Zimmerman.** 2002. Distinct patterns of downstream target activation are specified by the helix-loop-helix domain of proneural basic helix-loop-helix transcription factors. Dev. Biol. **247:**137–148.

72. **Theil, T., G. Alvarez-Bolado, A. Walter, and U. Ruther.** 1999. Gli3 is required for Emx gene expression during dorsal telencephalon development. Development **126:**3561–3571.

73. **Tole, S., C. W. Ragsdale, and E. A. Grove.** 2000. Dorsoventral patterning of the telencephalon is disrupted in the mouse mutant extra-toes(J). Dev. Biol. **217:**254–265.

74. **Tomita, K., K. Moriyoshi, S. Nakanishi, F. Guillemot, and R. Kageyama.** 2000. Mammalian achaete-scute and atonal homologs regulate neuronal versus glial fate determination in the central nervous system. EMBO J. **19:**5460–5472.

75. **von Frowein, J., A. Wizenmann, and M. Gotz.** 2006. The transcription factors Emx1 and Emx2 suppress choroid plexus development and promote neuro-epithelial cell fate. Dev. Biol. **296:**239–252.

76. **Watanabe, K., D. Kamiya, A. Nishiyama, T. Katayama, S. Nozaki, H. Kawasaki, Y. Watanabe, K. Mizuseki, and Y. Sasai.** 2005. Directed differentiation of telencephalic precursors from embryonic stem cells. Nat. Neurosci. **8:**288–296.

77. **Xu, Z. P., A. Dutra, C. M. Stellrecht, C. Wu, J. Piatigorsky, and G. F. Saunders.** 2002. Functional and structural characterization of the human gene BHLHB5, encoding a basic helix-loop-helix transcription factor. Genomics **80:**311–318.